

Critical Stresses for Microcracking in Monoclinic Zirconia

W. WUNDERLICH AND M. RÜHLE*

Max-Planck-Institut für Metallforschung
Institut für Werkstoffwissenschaften
7000 Stuttgart 1, Federal Republic of Germany

A complex twinned microstructure is observed in monoclinic (*m*) ZrO₂ after the martensitic transformation in ZrO₂ from the tetragonal (*t*) to the monoclinic (*m*) structure in skull-melted materials. Triangularly shaped twinned regions are formed where the thickness of the twin lamellas varies. At the end of the twin lamellas, strains (and stresses) develop which scale on the lamella thickness. If a critical strain level is surpassed, microcracks develop. HREM studies allow the determination of two-dimensional displacement fields near the end of the lamellas. Strain contours (and stress contours) of the different components are developed from the displacement fields. For the given geometry the analysis yields a maximum tensile strain of 0.14 and a shear strain of 0.05.

Microcracking within brittle ceramics requires that local stresses exceed a critical value. Microcracks may improve the properties of the mechanics, especially the toughness of a ceramic¹⁻³ or—if an uncontrolled growth of the microcracks occurs—those properties may also be deleterious. It is of great scientific and also practical interest to understand up to which level a ceramic material may sustain internal stresses until microcracking occurs. Furthermore, it is desirable to understand the mechanisms which lead to microcracking.

In this paper, examples are given for the possibility of evaluating the displacement and strain fields in a ceramic. Their critical value corresponds to the determined maximum strains. The evaluations are performed for monoclinic ZrO₂ (*m*-ZrO₂) from direct lattice images obtained by high-resolution electron microscopy (HREM).

Experimental Details

All studies were performed on skull-melted *m*-ZrO₂ crystals. No macroscopic cracks could be observed in the bulk crystal. The preparation of specimens suitable for TEM followed the standard routine.^{4,5} Thicknesses of ≤ 20 nm are required for HREM studies.

*Present address: Materials Department, College of Engineering, University of California at Santa Barbara, Santa Barbara, CA.

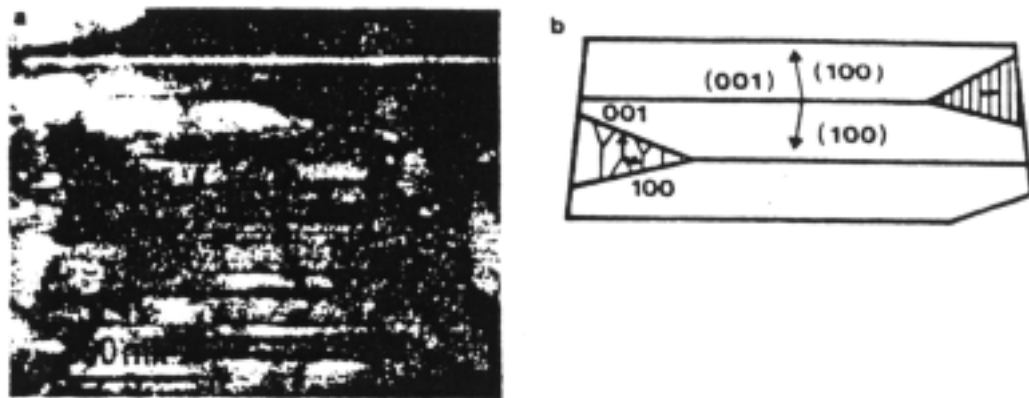


Fig. 1. (a) Low-magnification skull-melted m -ZrO₂ TEM micrograph. (b) Schematic of twinned structures. The interface between a large twin and a triangle is studied.

The TEM studies were performed in a high-resolution instrument which possesses a point-to-point resolution of 0.23 nm. The specimen was carefully adjusted so that the incoming electron beam coincided with a selected $\langle 010 \rangle$ zone axis of the specimen. Projectives of the perfect and the slightly bent unit cell of m -ZrO₂ (lattice parameter $a = 0.512$ nm, $b = 0.524$ nm, $c = 0.531$ nm, monoclinic angle $\gamma = 81^\circ$) can be measured directly and there exists a good agreement between the image and the projection of the crystal.

Experimental Observations

Skull-melted m -ZrO₂ contains a high density of different twins. The twins formed during the martensitic tetragonal (t)-to-monoclinic (m) transformation which occurs in bulk ZrO₂ at ≈ 1150 K. The twins reduce the strains resulting primarily from a shape change during transformation. These thick twin lamellae (see Fig. 1) possess a thickness of about 100 to 300 nm. Frequently, triangularly shaped regions can be observed at the end of such twins (Fig. 1). Probably the large triangle regions possessed orthorhombic symmetry^{6,10} and continued to transform on further cooling to m -ZrO₂, introducing twins and additional smaller triangles of orthorhombic ZrO₂. An example of a twinned triangular region is shown in Fig. 2(a). The crystallographic orientation relationships are represented in Fig. 2(b).

The two-dimensional defects in Fig. 2(a) are also (100) twins. The measured width of the lamella is 0.25 of its length. Either lattice bending (due to elastic strains) or microcracking occurs in the regions of intersection of the small twin with the surrounding m -ZrO₂ plates. The small triangles are present within the regions of compression. The latter observations may correspond to "domains of closure."^{7,10} The strained regions close to the terminating twins can be mapped by HREM for platelets of m -ZrO₂ with different thicknesses. The difference between the unstrained and the strained lattice results in a displacement field. The corresponding strains can be obtained by taking the appropriate derivatives. Maximum strains are expected for platelets with large thicknesses. A micrograph taken with higher magnification and resolution is shown in Fig. 3(a) and 3(b) is a drawing of the crystallographic orientation relationships. Figure 3(a) shows a micrograph of a corner of a twin boundary at a higher magnification. The bending of the lattice planes (resolved by HREM) can readily be observed in Fig. 3(a) if

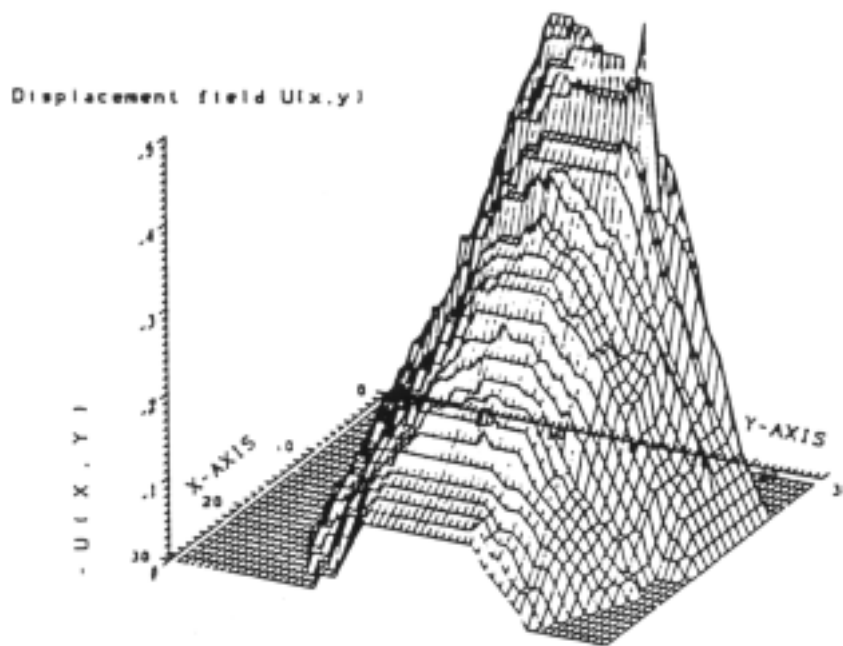


Fig. 4. Three-dimensional representation of the displacement field $u(x, y)$. The undisturbed mesh in the x - y plane corresponds to the m - ZrO_2 lattice. The units of $u(x, y)$ correspond to 0.1 nm.

Fig. 3(b). The displacement fields $u(x,y)$ and $v(x,y)$ can be measured. A direct evaluation from HREM images is possible and no change of the HREM image is expected since the lattice parameters of m - ZrO_2 are large compared to the point-to-point resolution of the TEM.

The displacement field $u(x,y)$ and $v(x,y)$ was evaluated for various regions near a terminating twin and the results for $u(x,y)$ and for one twin configuration are depicted in Fig. 4. The experimentally measured displacements are smoothed before derivatives are formed. The very thin foil used for the HREM studies represents a plane-stress configuration in a very good approximation. These strain components can be evaluated by

$$\epsilon_x = \frac{\partial u}{\partial x} \quad \epsilon_y = \frac{\partial v}{\partial y} \quad \epsilon_{xy} = \frac{1}{2} \left(\frac{\partial u}{\partial y} + \frac{\partial v}{\partial x} \right) \quad (1)$$

The experimentally evaluated components of the strain tensor are shown in Fig. 5(a) to (c). A comparison with the selected geometry shows that, as expected, the highest tensile strains ϵ_x are noticed close to the twin plane ($x = 0, y = 0$). The results of the displacement field for $u(x,0)$ for twin lamellas of four lamella thicknesses are shown in Fig. 6(a). Differentiation in the x direction leads to the strain ϵ_x .

The experimentally determined maximum tensile strain has a value of 0.14. Therefore, it is concluded that larger values lead to microcracking under the experimentally selected conditions, which is also observed (Fig. 2(a)).

Under the assumption that m - ZrO_2 represents an isotropic material, the determined maximum tensile stress can be calculated by

$$\sigma_x = \frac{E}{1 - \nu^2} [\epsilon + \nu\epsilon_y] \quad (2)$$

Assuming elastic values of $E = 200$ GPa and $\nu = 0.19^9$ results in a critical tensile stress

$$\sigma_x^c = 29 \text{ GPa} \quad (3)$$

for calculations concerning this material.

Discussion

The experimental results show that an $m\text{-ZrO}_2$ single crystal (in this case the matrix) can withstand large local strains. The strains and strain fields can be

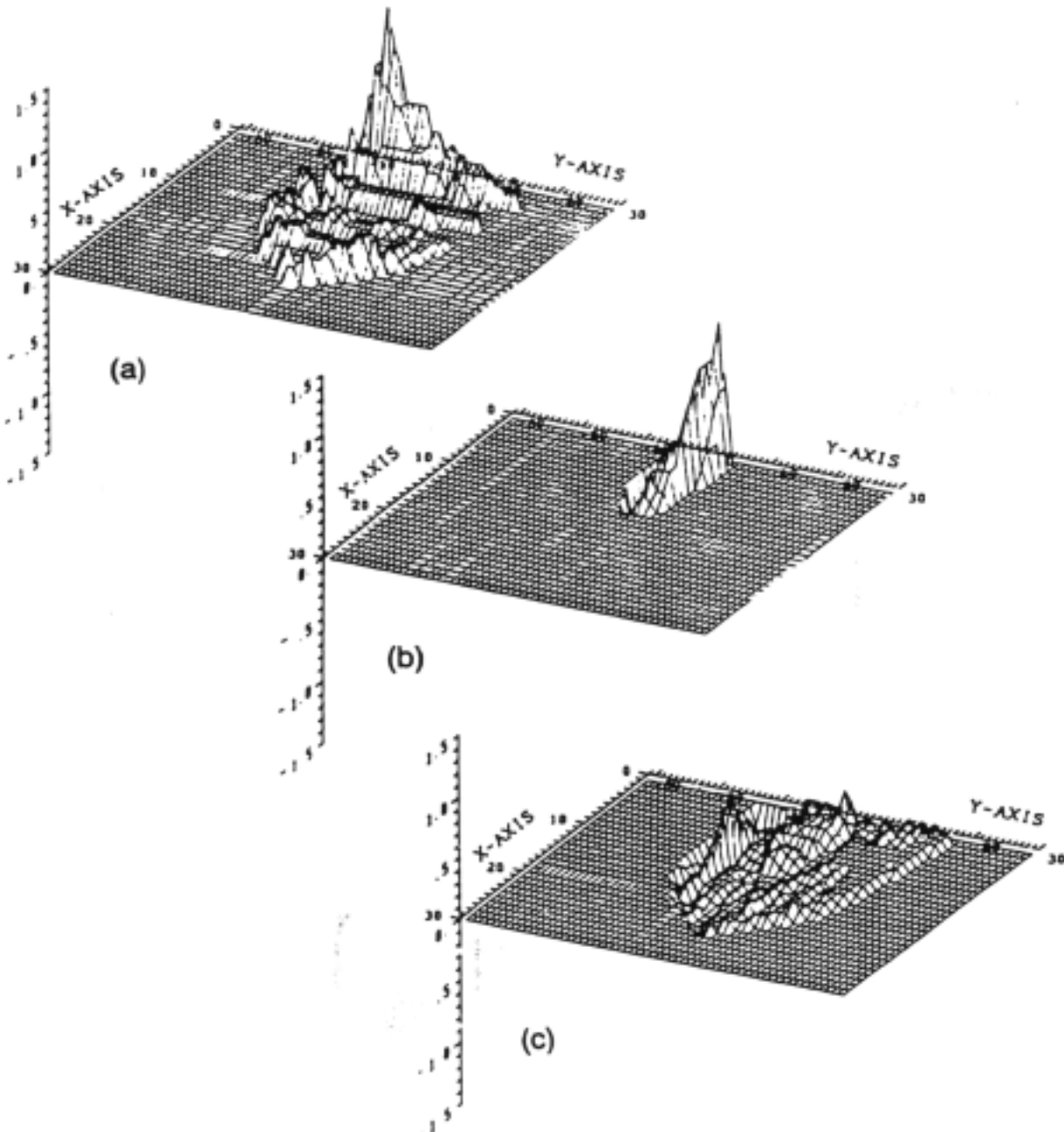


Fig. 5. Three-dimensional presentation of the three strain components of the strain tensor for plane stress configuration. The strain fluctuations are partially caused by errors due to the noise in the picture. (a) ϵ_{xx} component; (b) ϵ_{yy} component; (c) ϵ_{xy} component.

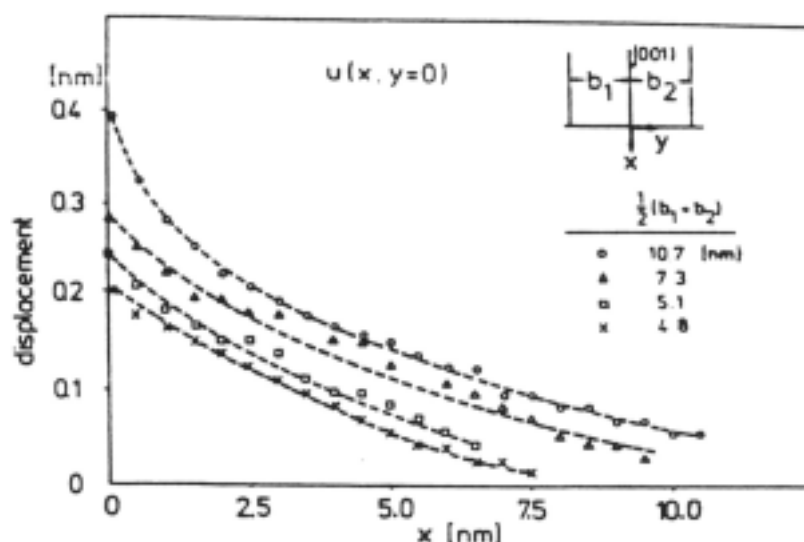


Fig. 6. The measured displacement field $u(x, 0)$ as a function of the distance from the interface. The symbols correspond to lamellas of different thicknesses.

measured by a quantitative evaluation of HREM images. Experimentally, it could be shown that the displacement field drops off with $r^{-1/2}$, r representing the distance from the mid-twin plane.

The rather high values of the strains obtained prior to microcracking also correspond to theoretical considerations. Microcracking in a totally bent material requires the breaking of atomic bonds. This is expected to take place at a critical stress level of $\sigma_x^c \approx 0.1E = 20$ GPa ($E =$ modulus of elasticity), in good agreement with the measured value. The critical stage is important for the design of microcrack-toughened ceramics.

Dislocations or disclinations near the mid-twin plane may reduce the internal stresses.¹⁰ However, these stresses may also reduce the stresses required for microcracking.

The experimental results can be compared to a theoretical model evaluated by Fu et al.,⁸ who analyzed the stress distribution at the ends of the twins for an m -ZrO₂ particle embedded in Al₂O₃ and composed of two or six twins. Using linear elasticity, they found that for very small microcracks the stress intensity factor dropped below the critical stress intensity factor for crack growth which had been estimated from experimentally determined crack lengths. They thus concluded that spontaneous initiation of very small microcracks cannot be explained by using linear elasticity and they suggested that microcrack nucleation requires the presence of lattice defects (for example, dislocations), or involves nonlinear bond displacement in response to the very high stress concentrations. The experimental observations presented in this paper support the latter model (cf. Fig. 3). With these results the data have to be reevaluated assuming the nonlinear theory.

References

- ¹A. G. Evans and K. T. Faber, "Crack-Growth Resistance of Microcracking Brittle Materials," *J. Am. Ceram. Soc.*, **67** [4] 255-60 (1984).
- ²A. G. Evans and K. Fu, "Some Effects of Microcracks on the Mechanical Properties of Brittle Solids—II. Microcrack Toughening," *Acta Metall.*, **33** [8] 1525-31 (1985).

³M. Rühle, A. G. Evans, R. M. McMeeking, P. G. Charalambides, and J. W. Hutchinson, "Microcrack Toughening in Zirconia Toughened Alumina," *Acta Metall.*, **35**, 2701-10 (1987).

⁴C. Springer and M. Rühle, "Präparation von keramischen Werkstoffen für die Durchstrahlungselektronenmikroskopie, Sonderbände der praktischen Metallographie"; p. 223 in Band 9, Metallographie und Keramografie. Edited by W. U. Kopp and H. E. Bühler. Dr. Riederer-Verlag GmbH, Stuttgart, 1978.

⁵A. Strecker, G. Necker and M. Rühle, "Concave Grinding Units (Dimpler) for Preparing Transmission Electron Microscope Specimens," *Pract. Metallographie*, **23**, 417-29 (1986).

⁶Y. H. Chiao and I. W. Chen, "In-situ TEM Observations of the Structures and Migration of Martensitic Interface in Small ZrO₂ Particles," *Trans. Jpn. Inst. Met.*, **27**, 197-203 (1986).

⁷E. Bischoff and M. Rühle, "Twin Boundaries in Monoclinic ZrO₂ Particles Confined in a Mullite Matrix," *J. Am. Ceram. Soc.*, **66** [2] 123 (1983).

⁸K. Fu, A. G. Evans, and W. M. Kriven, "Microcrack Nucleation in Ceramics Subject to a Phase Transformation," *J. Am. Ceram. Soc.*, **67** [9] 626-30 (1984).

⁹R. P. Ingel, "Structuremechanical Property Relationships for Single Crystal Y₂O₃ Stabilized ZrO₂"; Ph.D. Thesis, The Catholic University of America, Washington D.C., 1982.

¹⁰W. Wunderlich, "Spannungsanalyse an Zwillingen in Zirkoniumdioxid mit hochauflösender Elektronenmikroskopie"; Ph.D. thesis, Universität Stuttgart, 1987.